Kinetic processes in the transition from Ag(111) crystallites to $(\sqrt{3}\times\sqrt{3})R30°$ domains for Ag/Si(111)-(7×7)

J.-K. Zuo
Department of Physics and Astronomy, Southwest Missouri State University, Springfield, Missouri 65804

J. F. Wendelken
Solid State Division, Oak Ridge National Laboratory, Oak Ridge, Tennessee 37831

(Received 17 December 1996)

Kinetic processes in the transition from metastable Ag(111) crystallites to $(\sqrt{3}\times\sqrt{3})R30°$ domains in the initial growth of Ag on the Si(111)-(7×7) surface have been investigated using spot profile analysis low-energy electron diffraction. Upon annealing above 468 K, the number density $M(t)$ of metastable Ag(111) crystallites (deposited at $T_d\sim333$ K) is found to decrease exponentially with time t. Simultaneously, the average size of $\sqrt{3}$ domains increases as $R(t)\sim t^x$, with the exponent x increasing with initially deposited coverage and limited to a range of $1/3\leqslant x\leqslant 2/5$. A theoretical model for this structural transition is established to explain these observations, which is based on a kinetic process driven by the step-edge line tension of terraces in the Ag(111) crystallites. Also, a dissociation energy of an atom from the step edge of a Ag(111) crystallite is determined to be $E_{\rm dis}\sim1.38$ eV. [S0163-1829(97)01932-2]

I. INTRODUCTION

The growth of metals on semiconductors is an area of continuing interest due to its technological importance. Ag/Si(111), one of most studied metal-semiconductor systems, exhibits an abrupt interface with a very stable intermediate layer of the $(\sqrt{3}\times\sqrt{3})R30°$ structure (hereafter $\sqrt{3}$).[1–18] It is well known[1–4] that, for Ag deposited on the Si(111)-(7×7) surface at a temperature $T>468$ K, the two-dimensional (2D) $\sqrt{3}$ layer forms first, then stable 3D Ag(111) crystallites or islands will develop atop the $\sqrt{3}$ layer, i.e., following the Stranski-Krastanov growth mode. For deposition at $T<468$ K, metastable 3D Ag(111) islands grow directly on the (7×7) substrate surface without the initial $\sqrt{3}$ layer.[1–6] These metastable islands, upon annealing above 468 K, will partially dissolve to form the $\sqrt{3}$ structure until it saturates the surface, and the remaining islands then become stable due to the Stranski-Krastanov growth mechanism. This indicates that formation of the $\sqrt{3}$ structure has an activation energy which can be overcome at $T>468$ K.[3] However, results of recent experiments revealed that the $\sqrt{3}$ structure can also be formed by deposition of Ag onto the preformed Si(111)-(3×1)-Ag surface.[11] Although this system has been extensively investigated from the submonolayer to multilayer ranges, most work has been devoted to the atomic structure and saturation coverage of the $\sqrt{3}$ layer,[12–18] with little attention paid to kinetic processes in the structural transition from metastable 3D Ag(111) islands to the stable $\sqrt{3}$ structure upon annealing. Similar phenomena have also been observed for the growth of Au, Ta, Pt, Pd, and Al on Si(111).[1,7] Therefore, a study of kinetic processes in the structural transition for Ag/Si(111) is of general interest.

In this paper, we report our studies on kinetic processes and the driving force for the decay of metastable 3D Ag(111) islands and the corresponding growth of $\sqrt{3}$ domains, at different annealing temperatures and coverages, using spot-profile-analysis low-energy electron diffraction (SPA-LEED). We found that upon annealing above 468 K, the number density $M(t)$ of metastable Ag(111) crystallites deposited at $T_d\sim333$ K decreases with time t exponentially, and meanwhile the average size of $\sqrt{3}$ domains increases as $R(t)\sim t^x$, with the exponent x depending on coverage. These behaviors can be explained by a kinetic process which is driven by the step-edge line tension of Ag(111) crystallites consisting of multilevel terraces with curved step edges.

II. EXPERIMENTAL

Experiments were performed in an ultrahigh-vacuum chamber with a base pressure of 5.0×10^{-11} Torr. The chamber was equipped with a high-resolution SPA-LEED system, a double-pass cylindrical mirror analyzer for Auger electron spectroscopy (AES), and a 99.9999% pure Ag evaporator. The sample can be heated by a tungsten filament from the backside using either radiation heating or electron bombardment (with a high positive voltage applied to sample). The Si(111)-(7×7) surface was prepared by flashing (using electron bombardment) the sample to ~1250 °C and then slowly cooling down. After cleaning, no impurities were detected with AES. From the energy-dependent full width at half maximum (FWHM) of the (00) beam, the average terrace width on the clean Si(111)-(7×7) surface was determined to be ~1000 Å. Temperature was measured with a W5% Re–W6% Re thermocouple attached at an edge of the sample surface. In the experiments, we first deposited a desired coverage of Ag on the Si(111)-(7×7) surface at $T_d\sim333$ K to form metastable 3D Ag(111) islands, then raised the sample temperature (using radiation heating) slowly to slightly below ~468 K (no $\sqrt{3}$ structure appears at this point), and subsequently heated the sample quickly to and held it at a predetermined temperature T above 468 K. This up-quench procedure can minimize nonuniform heating

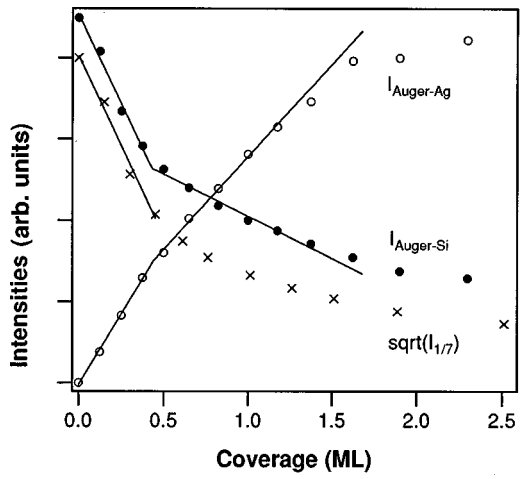

FIG. 1. A plot of the Auger Ag(MNN)(352 eV) and Si(LVV)(92 eV) peak-to-peak intensities and the square root of a 1/7-order peak intensity, vs coverage at a deposition temperature of 333 K. The solid lines are simply a visual guide.

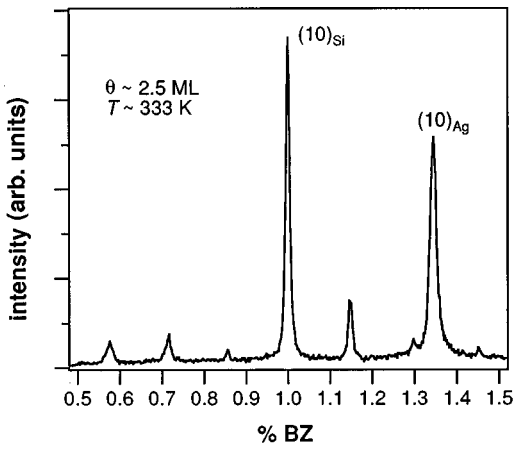

FIG. 2. A line scan of the diffraction pattern in the direction from the specular (00) peak (not shown in the left side) to the $(10)_{Si}$ or $(10)_{Ag}$ peak, where the small peaks are all 1/7-order peaks from the (7×7) surface. BZ is the Brillouin zone length from the (00) to $(10)_{Si}$ peaks.

of the Si sample. After the up-quenching, the $\sqrt{3}$ domains evolved, while the Ag(111) islands dissolved. The angular profile of a $\sqrt{3}$ superlattice diffraction beam and a Ag(111) diffraction beam were recorded with time to extract the kinetic features for both the $\sqrt{3}$ domain growth and the Ag(111) island dissolution. Because of its good spatial ($0.006\ \text{Å}^{-1}$) and time (ms) resolutions, SPA-LEED is particularly suitable for this kind of kinetic study. Three different coverages of $\theta\sim0.5$, 1.0, and 2.5 monolayers (ML) were used in the experiments. The coverage was calibrated by determining the break point in a plot of the Ag(MNN) $\times$(352 eV) or Si(LVV)(92 eV) Auger signals vs deposition time, and the break point in a similar plot for the total intensity of a $\sqrt{3}$ diffraction beam, at a deposition temperature of $T_d=723$ K. The three break points coincide in time and were assigned to be 1.0 ML.[3,4,13,15–18] The deposition rate was thus determined to be $F\sim0.15$ ML/min.

III. RESULTS AND DISCUSSIONS

A. Dissolution of metastable 3D Ag(111) islands

We first examine the coverage at which 3D Ag(111) islands start to form at the deposition temperature $T_d=333$ K. Figure 1 is a plot of the Auger Si(LVV)(92 eV) and Ag(MNN)(352 eV) peak-to-peak intensities, and the square-root of a 1/7-order diffraction peak intensity vs coverage θ at $T_d=333$ K. Initially, the Si Auger signal decreases and the Ag Auger signal increases linearly, and then both of them vary more slowly beyond a break point at $\theta_c\sim0.45$ ML. The same behavior occurs for the square root of the 1/7-order diffraction peak intensity which is a measure of the total exposed area of the (7×7) surface. The initial linear variations of these intensities imply a growth of 2D Ag(111) islands,[1] which is terminated at $\theta_c\sim0.45$ ML after which 3D Ag(111) islands develop. This result is consistent with that of other published measurements at room temperature.[1,5,6] Next, we present the kinetic data for the dissolution of metastable 3D Ag(111) islands upon annealing above 468 K. In order to obtain sufficient intensity for Ag(111) diffraction beams, data were acquired for a coverage of $\theta\sim2.5$ ML. After deposition at ~333 K, arc-shaped diffraction spots from rotationally degenerate twin Ag(111) crystallites were observed along with a weakened (7×7) substrate diffraction pattern. Shown in Fig. 2 is a line scan of the diffraction pattern in the vicinity of the $(10)_{Si}$ peak, containing the $(10)_{Ag}$ peak and some 1/7-order substrate peaks. The scan is along the radial direction from the specular (00) peak to the $(10)_{Si}$ peak. One of the rotationally degenerate Ag(111) crystallite types shows the epitaxial orientation of $[110]_{Ag}//[110]_{Si}$, whereas the other is just rotated 180° about the surface normal with respect to the first one. The arced shape of the Ag(111) diffraction spots implies a small orientational distribution of Ag(111) islands. The remaining (7×7) diffraction pattern indicates that Ag(111) crystallites grow in the form of 3D islands, which leave some residual (7×7) substrate exposed and undisturbed at $\theta\sim2.5$ ML. Figure 3 shows three sets of data for the peak intensity and FWHM of the $(10)_{Ag}$ peak vs annealing time t after up-quenching to different temperatures. A constant background has been subtracted from the intensity and the FWHM was measured perpendicular to the arc direction to eliminate the spreading effect due to the small orientational distribution of Ag(111) islands. An incident electron energy, $E_i=90$ eV, was chosen to be near the in-phase condition for scattering from different terraces separated by single atomic steps in the 3D Ag(111) island. In such a condition, the FWHM is inversely proportional to the average projected radius ρ of the Ag(111) island onto the surface, i.e., $\rho\propto1/\text{FWHM}$, and the peak intensity is given by

$$I_{(10)_{Ag}}(t)\propto M(t)\rho^4, \tag{1}$$

where $M(t)$ is the number density of Ag(111) islands. In Fig. 3 the nearly invariant FWHM with time indicates that ρ does not vary with time, so the decrease of $I_{(10)_{Ag}}$ with time must result from a decrease in $M(t)$ according to Eq. (1), i.e., $I_{(10)_{Ag}}\propto M(t)$. The constant ρ also suggests that Ag atoms dissolve layer by layer starting from the top of an island, while keeping the projected area of the island almost un-

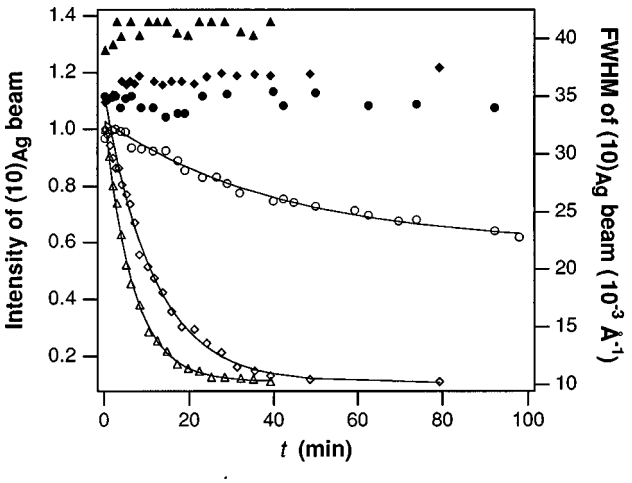

FIG. 3. The normalized peak intensity and FWHM of the $(10)_{Ag}$ beam vs annealing time for up-quench temperatures of ~473 K (circles), 488 K (diamonds) and 498 K (triangles). Open and solid symbols correspond to the left axis (intensity) and the right axis (FWHM), respectively. The solid curves are the least-squares fits of Eq. (2) to the peak intensities.

changed (see the schematic in Fig. 4). The dissociated atoms diffuse downward from the upper island terraces until reaching the Si surface to form the $\sqrt{3}$ structure surrounding the island. This process proceeds until the island reduces to one layer thick after which the island collapses. Ultimately, a saturated coverage of the $\sqrt{3}$ structure is reached, and residual Ag(111) islands become stable because of the Stranski-Krastanov growth nature. To quantitatively describe the time dependence of $I_{(10)_{Ag}}$, we can set up a rate equation, $dM/dt = -\lambda[M(t) - M(\infty)]$, where $M(\infty)$ is the residual stable island density and λ is a kinetic coefficient. This equation implies that the decay rate of M is proportional to the net unstable island density. Its solution is

$$I_{(10)_{Ag}} \propto M(t) = M(\infty) + [M(0) - M(\infty)]\exp(-\lambda t). \quad (2)$$

The solid curves in Fig. 3 are the least-squares fits of Eq. (2) to the peak intensities. The excellent fits give $\lambda = 0.024$, 0.086, and 0.158 for up-quench temperatures of $T = 473$, 488, and 498 K, respectively. A slight deviation from the data at initial times is due to the fact that at the beginning every island has a finite thickness and cannot disappear immediately. If we let $\lambda \propto \exp(-E_\lambda/k_B T)$, the decay energy E_λ is determined from an Arrhenius plot to be 1.53 ± 0.03 eV.

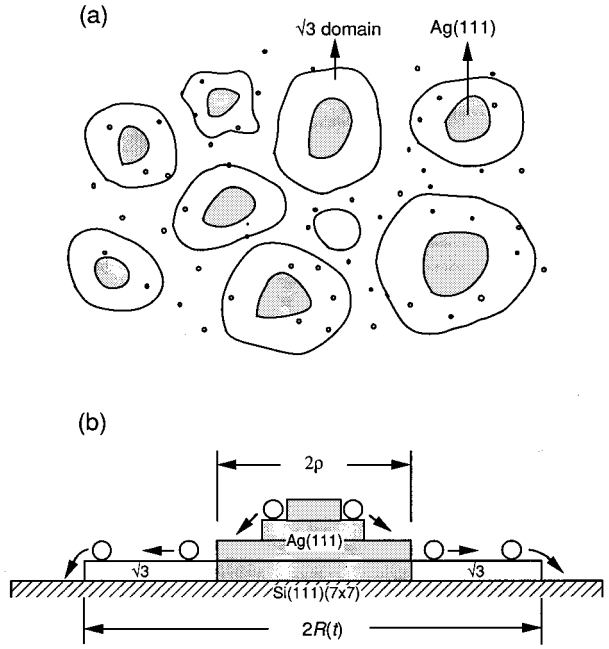

FIG. 4. A schematic picture of (a) and the Ag(111) island distribution and (b) individual Ag(111) island dissolution with the corresponding $\sqrt{3}$ domain growth on the Si(111)-(7×7) surface during annealing.

B. Growth of $\sqrt{3}$ domains

While Ag(111) islands are dissolving upon annealing as discussed above, $\sqrt{3}$ domains are evolving. This is observed by monitoring the (1/3, 1/3) superlattice diffraction beam of the $\sqrt{3}$ structure. Since the average $\sqrt{3}$ domain size is $R \propto 1/\mathrm{FWHM}$ of the (1/3, 1/3) angular profile, the growth law for the $\sqrt{3}$ domain may be determined experimentally. We found that a form

$$R(t)^2 - R(0)^2 = A(T)t^{2x}, \quad (3)$$

can describe our data well, where $A(T)$ is a temperature-dependent factor, and $R(0)$ is the initial domain size just after up-quenching (after a predetermined up-quench temperature is reached, a small $\sqrt{3}$ domain surrounding each Ag(111) island will normally be formed due to a finite quenching time). By considering $R(t) \propto 1/\mathrm{FWHM}(t)$, the data and fits of Eq. (3) are plotted in Figs. 5(a), 5(b), and 5(c) for $\theta \sim 0.5$, 1.0, and 2.5 ML, respectively, with each coverage repeated at different up-quench temperatures. The average exponents for each coverage are determined to be $2x = 0.69 \pm 0.03$, 0.74 ± 0.03, and 0.78 ± 0.03, accordingly, which *increase* with increasing coverage. For $R(t) \gg R(0)$ after a short annealing time, we actually have $R(t) \sim t^x$ with $x \sim 0.35$, 0.37, and 0.39, respectively.

In the following we will explain the microscopic origin of this growth law which sheds light on the decay mechanism of 3D Ag(111) islands. Two conceivable processes might be responsible for the growth behavior. The first one is the Lifshitz-Slyozov coarsening,[19] i.e., the growth is due to mass transport among existing $\sqrt{3}$ domains in which large domains grow at the expense of small ones. The second one is the attachment of atoms which are dissociated from the Ag(111) islands, to the perimeter of the $\sqrt{3}$ domain surrounding the Ag(111) island, see Fig. 4. In order to distinguish these two processes, we have measured the time dependences of the peak intensity $I_{1/3}$ of the (1/3, 1/3) beam and the peak intensity $I_{(10)_{Ag}}$ of the $(10)_{Ag}$ beam at $\theta \sim 2.5$ ML and $T \sim 498$ K. As can be seen in Fig. 6, the increase in $I_{1/3}$ and the decrease in $I_{(10)_{Ag}}$ are almost synchronized, and they level off at about the same time. This clearly indicates that the atom supply for the $\sqrt{3}$ domain growth is atoms dissociated from the Ag(111) islands, i.e., the second process described above is the dominating process. If the $\sqrt{3}$ domain growth were due to the Lifshitz-Slyozov coarsening, we would expect that the growth should continue after the decay of

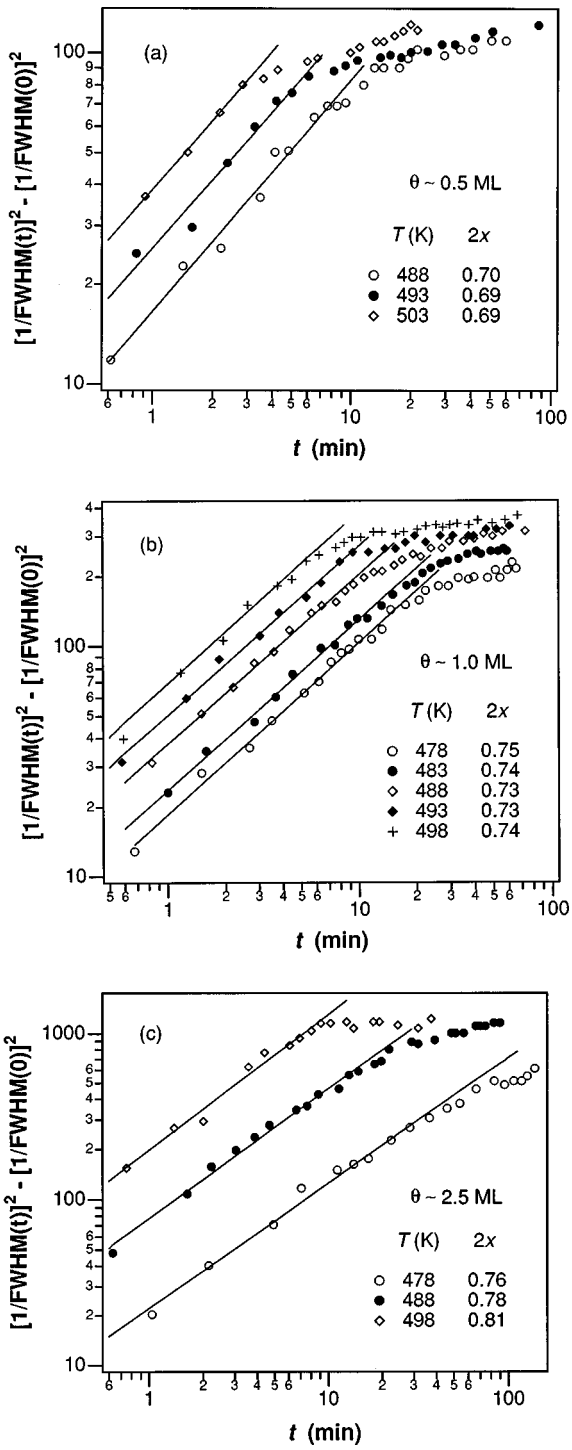

FIG. 5. FWHM of the (1/3, 1/3) beam plotted vs annealing time t in a manner consistent with Eq. (3) and $R(t) \propto 1/\mathrm{FWHM}(t)$. Three data sets are shown for (a) $\theta = 0.5$ ML, (b) $\theta = 1.0$ ML, and (c) $\theta = 2.5$ ML, with each coverage repeated at different up-quench temperatures. Solid lines are the least-squares fits of Eq. (3) to the data, and the slope gives the exponent $2x$.

Ag(111) islands has stopped, and also the exponent should stay at $x = 1/3$ independent of coverage. Now, the remaining question is why the second process will result in a growth obeying Eq. (3) with x increasing with increasing coverage. We will answer this question in the following.

As observed by scanning electron microscopy[2] and scanning tunneling microscopy,[6] the Ag(111) island has a quasi-

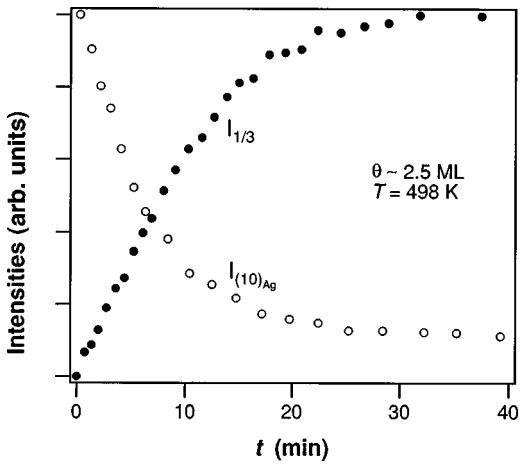

FIG. 6. Peak intensities of the $(10)_{\mathrm{Ag}}$ beam and (1/3, 1/3) beam are plotted vs annealing time t to display the simultaneous variations for the decay of Ag(111) islands and the growth of $\sqrt{3}$ domains.

hexagonal shape with round corners. So, the island can be viewed as consisting of multilevel terraces separated by single atomic steps with curved step edges, see Fig. 4. The step free energy can be written in the Gibbs-Thomson form, $\mu = \mu_0 + \sigma/r$,[20] where μ_0 is the straight step free energy, σ is the step-edge line tension, and r is the effective terrace radius. In order to lower the step free energy, atoms will be driven to migrate from an upper-terrace edge with a smaller radius to a lower-terrace edge with a larger radius, forming a downhill current. After reaching a steady downhill current which balances the loss due to dissociation at each terrace level, the radii of the lower terraces remain constant. Dissociation from the topmost terrace is not balanced by any source of atoms, therefore, the Ag(111) islands dissolve in a layer-by-layer fashion. This picture is consistent with the decay data of Ag(111) islands as discussed above. Assume that N terraces have disappeared in time t after the up-quench. According to the mass conservation law, we have that the sum of areas of the vanished terraces of a Ag(111) island equals the expanded area of the surrounding $\sqrt{3}$ domain, i.e.,

$$\pi[R(t)^2 - R(0)^2] = c\pi \sum_{i=1}^{N} r_i^2 \approx c\pi \int_0^{r_N(t)} r^2 dz$$

$$= c\pi \int_0^{r_N(t)} r^2 (r dr/\Re) = \frac{c\pi}{4\Re} r_N(t)^4, \tag{4}$$

where c is a geometric factor due to the difference between the $\sqrt{3}$ and (111) structures and the integration is a good approximation for the summation when $N \gg 1$. Also, for $N \gg 1$ we have assumed that the initial shape of the 3D Ag(111) island is a part of a sphere with radius $\Re$, so that $z \sim r^2/2\Re$ for $r \ll \Re$ in a cylindrical coordinate system with the origin set at the initial top of the sphere and the z axis pointing downward. Now, we will find $r_N(t)$ as a function of the total elapsed time t. Villain has shown[21] that the time spent for a top terrace of radius r_i to disappear is $t_i = r_i^3/K\sigma$, where $K \sim (1/T)\exp(-E/k_B T)$ is a kinetic coefficient with E being a characteristic energy which will be dis-

cussed in more detail later. Thus, the total elapsed time t after the up-quench for N terraces to disappear is

$$t=\sum_{i=1}^{N} t_i=\frac{1}{K\sigma}\sum_{i=1}^{N} r_i^3\approx\frac{1}{K\sigma}\int_0^{r_N(t)} r^3 dz$$

$$=\frac{1}{K\sigma}\int_0^{r_N(t)} r^3(rdr/\Re)=\frac{1}{5K\sigma\Re}\,r_N(t)^5. \qquad (5)$$

This relation is similar to one obtained by Uwaha[22] with a different prefactor. We will now discuss two extreme cases. For the first case, if the initial Ag(111) island is only one layer thick as in our case of $\theta\sim 0.5$ ML, $N=1$ in Eqs. (4) and (5). In this case we just need to take the first term in these summations and obtain Eq. (3) with $x=1/3$. The second case, $N\gg 1$, occurs if the initial Ag(111) island is thick. In this case we take the results after integration in Eqs. (4) and (5), and then combine them to obtain Eq. (3) with $x=2/5$. No matter which case, the temperature-dependent factor $A(T)$ in Eq. (3) can be expressed as

$$A(T)\propto\frac{1}{T^{2x}}\exp(-2xE/k_BT). \qquad (6)$$

In our experiments with the coverages used, the thickness of the Ag(111) islands ranges between these two extreme cases, and hence an exponent of $1/3\leqslant x\leqslant 2/5$ is expected, which increases with increasing coverage or thickness. This is exactly what we have observed here, i.e., $x\sim 0.35$, 0.37, and 0.39 for $\theta\sim 0.5$, 1.0, and 2.5 ML, respectively.

Finally, we determine the characteristic energy E in Eq. (6) using the values of $A(T)$ obtained in the data fits shown in Fig. 5. In the decay process of 3D Ag(111) islands, the possible controlling energies are the dissociation energy $E_{\rm dis}$ of an atom from the terrace edge, the diffusion barrier $E_{\rm dif}$ on terraces and the step-edge barrier E_s which resists step-down diffusion. Thus we have $E=E_{\rm dis}+E_{\rm dif}+E_s$. Shown in Fig. 7 is an Arrhenius plot for the data of $\theta\sim 1$ ML and the fit of Eq. (6) with $2x\sim 0.74$. From the slope we obtained $E=1.93\pm 0.08$ eV. The diffusion barrier has been determined to be $E_{\rm dif}\sim 0.40$ eV by measuring the spreading of a patched Ag(111) island on the Si(111)-(7×7) surface at $650<T<750$ K.[3] The step-edge barrier for Ag/Ag(111) is measured to be $E_s\sim 0.15$ eV at room temperature[23] and ~ 0.12 eV at $T<150$ K.[24] Therefore, the average dissociation energy from step edge may be estimated to be $E_{\rm dis}\sim 1.38$ eV if we take $E_s\sim 0.15$ eV.

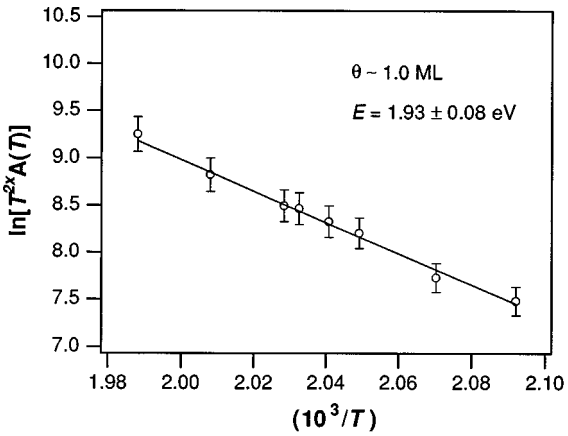

FIG. 7. An Arrhenius plot of $\ln[T^{2x}A(T)]$ vs $1/T$ allows determination of the characteristic energy E for the data of $\theta\sim 1$ ML according to Eq. (6) with $2x\sim 0.74$. The values of $A(T)$ are obtained from the data fits shown in Fig. 5(b).

IV. SUMMARY

Using SPA-LEED, we have studied kinetic processes in the transition from metastable Ag(111) crystallites to $\sqrt{3}$ domains in the initial growth of Ag on the Si(111)-(7×7) surface. We found that upon annealing above 468 K, the density $M(t)$ of metastable Ag(111) crystallites (deposited at $T_d\sim 333$ K) decreases with time t exponentially. At the same time, the average size of $\sqrt{3}$ domains increases as $R(t)\sim t^x$, with the exponent x increasing with coverage and limited to a range of $1/3\leqslant x\leqslant 2/5$. These observations have been explained by establishing a theoretical model based on a kinetic process which is driven by the step-edge line tension of multilevel terraces in vanishing Ag(111) crystallites. Also, we have obtained a dissociation energy of an atom from the step edge of Ag(111) crystallites to be $E_{\rm dis}\sim 1.38$ eV.

ACKNOWLEDGMENT

Work by J.F.W. was supported by the Division of Materials Sciences, U.S. Department of Energy under Contract No. DE-AC05-96OR22464 with Lockheed Martin Energy Research Corporation.

[1] G. Le Lay, M. Manneville, and R. Kern, Surf. Sci. **72**, 405 (1978); G. Le Lay, *ibid.* **132**, 169 (1983).
[2] J. A. Venables, J. Derrien, and A. P. Janssen, Surf. Sci. **95**, 411 (1980); M. Hanbücken, M. Futamoto, and J. A. Venables, *ibid.* **147**, 433 (1984).
[3] G. Raynerd, T. N. Doust, and J. A. Venables, Surf. Sci. **261**, 251 (1992); G. Raynerd, M. Hardiman, and J. A. Venables, Phys. Rev. B **44**, 13 803 (1991).
[4] S. Hasegawa, H. Daimon, and S. Ino, Surf. Sci. **186**, 163 (1987).
[5] E. J. Van Loenen, M. Iwami, R. M. Tromp, and J. F. Van der Veen, Surf. Sci. **137**, 1 (1984).
[6] St. Tosch and H. Neddermeyer, Phys. Rev. Lett. **61**, 349 (1988).
[7] W. S. Yang, S. C. Wu, and F. Jona, Surf. Sci. **169**, 383 (1986).
[8] J.-K. Zuo and J. F. Wendelken, Phys. Rev. Lett. **66**, 2227 (1991); J. Vac. Sci. Technol. A **9**, 1539 (1991).
[9] K. R. Roos and M. C. Tringides, Phys. Rev. B **47**, 12 705 (1993).
[10] H. Hong, R. D. Aburano, D.-S. Lin, H. Chen, T.-C. Chiang, P. Zschack, and E. D. Specht, Phys. Rev. Lett. **68**, 507 (1992).
[11] H. H. Weitering, N. J. DiNardo, R. Perez-Sandoz, J. Chen, and E. J. Mele, Phys. Rev. B **49**, 16 837 (1994); J. M. Carpinelli and H. H. Weitering, *ibid.* **53**, 12 651 (1996).
[12] R. J. Wilson and S. Chiang, Phys. Rev. Lett. **58**, 369 (1987); **59**, 2329 (1987).
[13] E. J. van Loenen, J. E. Demuth, R. M. Tromp, and R. J. Hamers,

Phys. Rev. Lett. **58**, 373 (1987).
[14] E. L. Bullock, G. S. Herman, M. Yamada, D. J. Friedman, and C. S. Fadley, Phys. Rev. B **41**, 1703 (1990).
[15] T. Takahashi, S. Nakatani, N. Okamoto, T. Ishikawa, and S. Kikuta, Jpn. J. Appl. Phys. **127**, L753 (1988).
[16] Y. G. Ding, C. T. Chan, and K. M. Ho, Phys. Rev. Lett. **67**, 1454 (1991).
[17] R. S. Daley, R. M. Charatan, and R. S. Williams, Surf. Sci. **240**, 136 (1990); M. Katayama, R. S. Williams, M. Kato, E. Nomura, and M. Aono, Phys. Rev. Lett. **66**, 2762 (1991).
[18] J. C. Woicik, T. Kendelewicz, S. A. Yoshikawa, K. E. Miyano, G. S. Herman, P. L. Cowan, P. Pianetta, and W. E. Spicer, Phys. Rev. B **53**, 15 425 (1996).
[19] I. M. Lifshitz and V. V. Slyozov, J. Phys. Chem. Solids **19**, 35 (1961).
[20] F. Lançon and J. Villain, in *Kinetics of Ordering and Growth at Surfaces*, edited by M. G. Lagally (Plenum, New York, 1990), p. 369.
[21] J. Villain, Europhys. Lett. **2**, 531 (1986).
[22] M. Uwaha, J. Phys. Soc. Jpn. **57**, 1681 (1988).
[23] J. Vrijmoeth, H. A. van der Vegt, J. A. Meyer, E. Vlieg, and R. J. Behm, Phys. Rev. Lett. **72**, 3843 (1994).
[24] K. Bromann, H. Brune, H. Roder, and K. Kern, Phys. Rev. Lett. **75**, 677 (1995).